Bubble growth and droplet decay in the quark-hadron phase transition in the early Universe

K. Kajantie
Department of Theoretical Physics, University of Helsinki and Academy of Finland, Siltavuorenpenger 20 C, SF-00170 Helsinki, Finland

Hannu Kurki-Suonio
Center for Relativity, University of Texas, Austin, Texas 78712
(Received 2 June 1986)

When the Universe was about 10 μsec old, it underwent a phase transition in which the quarks and gluons condensed into hadrons. We assume that this phase transition was of first order and study how the Universe evolved through the mixed phase in a scenario with small initial supercooling and monotonically growing hadronic bubbles. Nucleation of bubbles, collisions of shock fronts preceding the bubbles, arrestation of bubble growth by the reheating due to these collisions, subsequent slow growth of the bubbles to fill the entire Universe, condensation of baryon number, death of the remaining quark matter droplets, and the resulting density perturbations are discussed. A $(1+1)$-dimensional approximation is frequently used to make analytic calculations possible.

I. INTRODUCTION

It is quite probable that QCD matter can exist in two phases: a color-nonconfining quark-gluon plasma phase and a color-confining hadron phase. This conclusion is well established for pure glue matter with numerical lattice Monte Carlo calculations and even the order of the phase transition is then known to be one.[1] When quarks are included, the computations are essentially more complicated and the conclusions at present are only preliminary.

For physical applications of the quark-hadron phase transition, such as the early Universe[2–14] (big bang) or ultrarelativistic nucleus-nucleus collisions[1,15–25] (little bang) the situation is more complicated since not only is the equation of state needed but also knowledge of the kinetics of the phase transition. This is a notoriously difficult problem even in classical statistical physics. In the context of the QCD phase transition one can only formulate various scenarios, and cannot perform reliable calculations as in the context of cosmic synthesis of the light elements in the 1–100-sec-old Universe.

Depending on the amount of supercooling assumed one can distinguish between different scenarios: (1) no supercooling and no phase separation (see Refs. 2 and 3 for big bang and Refs. 17–21 for little bang); (2) small supercooling and phase separation (see Refs. 9 and 12 for big bang and Ref. 25 for little bang); (3) large supercooling (see Refs. 7–9 for big bang, and Refs. 22 and 23 for little bang). The more supercooling there is, the more spectacular the consequences can be expected to be. However, even the small-supercooling scenarios may leave relics of the cosmic transition as yet.[9]

The purpose of this paper is to study the small-supercooling–phase-separation scenario of Witten [big bang (BB)] and Van Hove [little bang (LB)] in some detail further. This scenario assumes that after an initial period of small supercooling the matter separates into hadron bubbles and quark droplets, the droplets having a larger energy density than the bubbles (by a factor of 3 in BB, about 10 in LB). The entire system can then expand at constant temperature and pressure by converting matter from the quark to the hadron phase by surface deflagration. This continues until all the matter is converted into the hadron phase and cooling resumes. In the cosmic context the energy transfer may also take place via radiation of neutrinos and leptons, which leads to enrichment of net baryon number.[9,12]

In the following we shall first in Sec. II study a simple model equation of state describing a first-order phase transition, both for zero and nonzero net baryon number. This will permit one to perform many of the later calculations analytically. Section III contains a discussion of the simplest way of going through the phase transition: after the Universe has cooled to the transition temperature T_c, the temperature simply stays there and the Universe goes on expanding by converting more and more quark matter to hadron matter with no phase separation. The relative amount of hadron matter $h(t)$ and the radius $R(t)$ are determined by Einstein's equations. These will serve as a framework on which the discussions of scenarios with more supercooling will be built.

Section III makes no assumptions about how the hadron matter is nucleated in the cosmic fluid. This is done in Sec. IV, containing a discussion of the initial thermal nucleation of hadron bubbles after the cosmic fluid has cooled slightly below the transition temperature T_c. As such, this theory would lead to an improbable result: the Universe would be filled with hadron matter in a superheated state much too rapidly. Instead, what perhaps happens is that the growth of the hadron bubbles is arrested, since the Universe between the hadron bubbles may be reheated to T_c by collisions of the shock fronts preceding the bubbles. This will be discussed in Sec. V. It appears that it is difficult to hit precisely the value T_c.

An important by-product of the discussion in Sec. IV is

the appearance of a new scale in the problem:[7] the average distance R_i between the bubbles after the slow growth starts. Many of the later results will depend on the ratio χR_i between R_i and the Hubble distance $1/\chi$. The larger the initial supercooling, the larger R_i and the final value of the numerical results will be. A van der Waals-type law of corresponding states leads to a reference value $R_i = 1$ m so that $\chi R_i \approx 10^{-4}$.

Section VI discusses what can be said about the growth just by using entropy conservation. Essentially, the required entropy flux from the quark-to-hadron regions is seen to be $T_c^3 \chi R_i$. Section VII will discuss the case when this flux is dominantly caused by a hydrodynamic flux of matter across the boundary. Going through the entire transition one sees that energy density inhomogeneities proportional to χR_i will remain at positions between the original bubbles.

A very important issue in this context is the behavior of baryon number.[9] This is quantitatively analyzed in Sec. VII. We point out that the formation and survival of the quark nuggets are connected in the sense that if they can be formed, they should also easier survive.

In the following we shall use a $(1+1)$-dimensional approximation whenever physically reasonable. This permits one to perform analytic calculations in many cases. Corrections due to the three dimensionality of the problem are finally estimated in Sec. IX.

This paper is limited to the discussion of the small-supercooling scenario with $\chi R_i \ll 1$ (and in the limit $R_i \to 0$ to the entirely homogeneous scenario). The possible consequences are thus not very easy to observe. In contrast, scenarios with large supercooling and χR_i near 1 would lead to spectacular consequences, but this large value of χR_i is hard to motivate.

II. EQUATION OF STATE

A necessary ingredient for any quantitative discussion of the phase transition is an explicit form for the equation of state. We shall use the simplest possible form of an equation of state incorporating a first-order phase transition: a bag equation of state. This has often been used for the zero-baryon-number case[8,19–25] and also extended to the case of any baryon number.[26–28] As the baryon-to-entropy ratio is very small in the cosmological case (unless the enrichment[9] is extreme), we shall limit ourselves to the case $\mu \ll T$. The physical foundation of an equation of state of this type is discussed in the references above and will not be repeated here.

Giving the equation of state is equivalent to giving the pressure ($=-$grand potential$/V$) as a function of T and μ. In the quark phase we have

$$p_q(T,\mu) = aT^4 + \tfrac{1}{18} N_F \mu^2 T^2 - B \ , \tag{2.1}$$

where

$$a = g_q \frac{\pi^2}{90} \ , \qquad g_q = 16 + \frac{21}{2} N_F + 14.25 = 51.25 \ , \tag{2.2}$$

and B is the bag constant ($=780$ MeV/fm^3 corresponding to $T_c = 200$ MeV in the numerical examples to follow). We use $N_F = 2$, although $N_F = 2.5$ might be quantitatively better to simulate the effect of the strange-quark mass. From p_q we obtain

$$\begin{aligned} s_q(T,\mu) &= \frac{dp_q}{dT} = 4aT^3 + \tfrac{1}{9} N_F \mu^2 T \ , \\ n_q(T,\mu) &= \frac{dp_q}{d\mu} = \tfrac{1}{9} N_F \mu T^2 \ , \\ \epsilon_q(T,\mu) &= 3aT^4 + \tfrac{1}{6} N_F \mu^2 T^2 + B \ . \end{aligned} \tag{2.3}$$

Note that here and in the following n denotes the net baryon-number density with a subscript q or h specifying the phase and μ is the associated chemical potential. Thus n_q is the baryon-number density in the quark phase and not the quark-number density and we do not have separate chemical potentials for quarks and baryons.

In the hadron phase we take the fluid to consist of an ideal gas of massless pions and of nucleons with Maxwell-Boltzmann statistics. Then

$$p_h(T,\mu) = a_\pi T^4 + b(m,T) T \cosh(\mu/T) \ , \tag{2.4}$$

where

$$a_\pi = g_h \frac{\pi^2}{90} \ , \qquad b(m,T) = \left(\frac{2mT}{\pi} \right)^{3/2} e^{-m/T} \ . \tag{2.5}$$

Numerically, for $m = 0.94$ GeV

$$\begin{aligned} b(m,T)/T^3 &= 0.047 \quad (T = 0.2 \text{ GeV}) \\ &= 0.020 \quad (T = 0.16 \text{ GeV}) \ . \end{aligned}$$

From p_h we further calculate

$$\begin{aligned} s_h(T,\mu) &= 4a_\pi T^3 + \left(\frac{5}{2} + \frac{m}{T} - \frac{\mu}{T} \tanh \frac{\mu}{T} \right) \cosh \frac{\mu}{T} \ , \\ n_h(T,\mu) &= b(m,T) \sinh \frac{\mu}{T} \ , \\ \epsilon_h(T,\mu) &= 3a_\pi T^4 + b(m,T) \left(m + \frac{3T}{2} \right) \cosh \frac{\mu}{T} \ . \end{aligned} \tag{2.6}$$

The critical curve $T = T_c(\mu)$ now is determined from $p_q(T,\mu) = p_h(T,\mu)$ (Figs. 1 and 2). As the phase transition is of first order, all the quantities s, n, and ϵ exhibit discontinuities across the critical curve. Figure 3 shows the discontinuity in n. The jump in n is given by

$$\begin{aligned} \frac{n_{qc}}{n_{hc}} &= \frac{N_F}{9} \frac{T_0^3}{b_0} = 5 \quad (T_0 = 0.2 \text{ GeV}) \\ &= 11 \quad (T_0 = 0.16 \text{ GeV}) \ , \end{aligned} \tag{2.7}$$

where

$$T_0 = T_c(0), \quad b_0 = b(m,T_0) \ .$$

Including terms of order μ^2/T^2 it is easy to derive approximations for the critical quantities. One has, for instance,

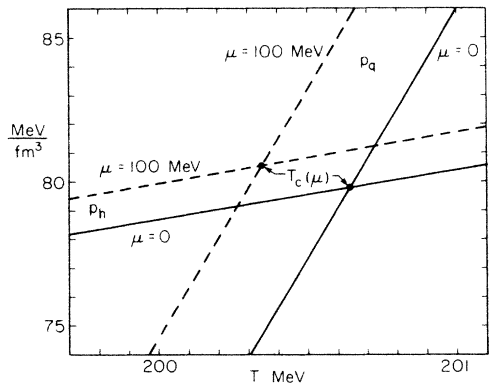

FIG. 1. Solving the critical curve $T=T_c(\mu)$ from the equilibrium condition $p_q(T,\mu)=p_h(T,\mu)$ for $\mu=0$ and 100 MeV with p_q and p_h given by Eqs. (2.1) and (2.4). The parameters are $T_c=200$ MeV, $g_q=51.25$, $g_h=17.25$, and B as given by Eq. (2.10). Note that $T_0=T_c(0)=200.64$ MeV due to the contribution of nucleons.

$$T_c(\mu)=T_0\left[1-\frac{N_F/18-b_0/2T_0^3}{a-a_\pi-b_0/T_0^3}\frac{\mu^2}{T_0^2}\right], \tag{2.8}$$

$$p_c[T_c(\mu)]=p_{c0}+\frac{ab_0/2T_0^3-a_\pi-b_0/T_0^3}{a-a_\pi-b_0/T_0^3}T_0^2\mu^2 .$$

For later purposes we shall also need those values of T and μ for which the pressure of the quark phase is the same as the pressure of the hadron phase at the transition temperature for $\mu=0$, i.e., the solution of $p_q(T,\mu)=p_{c0}$. This is also shown in Fig. 2 as the curve $T_{pc}(\mu)$. As $p_c(\mu)$ increases with μ, the curve T_{pc} lies below T_c.

In the early Universe $\mu/T=10^{-9}$ (without enrichment) and to a very good approximation one can set $\mu=0$ in the above. Then the contribution of the nucleon pressure in Eq. (2.4) is just a few percent and even it can be neglected. In this approximation we further have the following simple relations for the critical quantities:

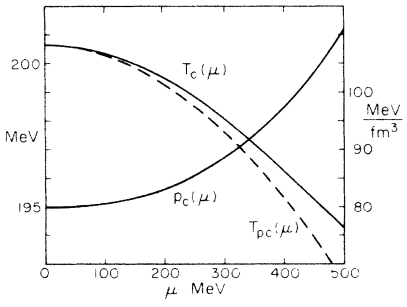

FIG. 2. The figure shows the μ dependence of the critical curve $T=T_c(\mu)$, the curve $T=T_{pc}(\mu)$ along which the pressure of the quark phase is the same as the pressure of the hadron phase at $\mu=0$ (needed in the discussion of enrichment of baryon number in quark droplets) and the pressure $p=p_c(\mu)$ along the critical curve. Parameters as in Fig. 1.

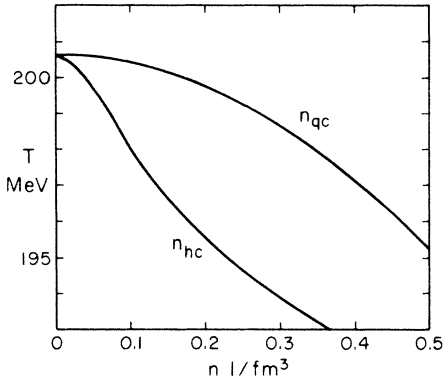

FIG. 3. The net baryon-number densities $n_{qc}(T)$ and $n_{hc}(T)$ along the critical curve. Parameters as in Fig. 1.

$$\frac{s_Q}{s_H}=\frac{w_Q}{w_H}=\frac{g_q}{g_h},$$
$$\epsilon_Q=\epsilon_H+4B, \tag{2.9}$$
$$\epsilon_H=\frac{3B}{r-1},$$

where $s_Q=s_q[T_c(\mu=0)]$, etc., and $w=\epsilon+p$ is the enthalpy. Also the relation between the bag constant and the transition temperature is simple:

$$B=(g_q-g_h)\frac{\pi^2}{90}T_c^4 . \tag{2.10}$$

III. THE FAST NUCLEATION AND NO-PHASE SEPARATION SCENARIO

We first go through the phase transition by assuming that everything is as smooth as possible: no supercooling and a uniform mixture of quark and hadron matter in the mixed phase.[3] This means that when the Universe has cooled down to $T=T_c$ and tries to cool further, regions of hadron matter start immediately forming. The latent heat released prevents further cooling and the Universe continues expanding maintaining $T=T_c$, $p=p_c$, and the constancy of the total entropy content by converting more and more of the matter from the dense quark phase to the less-dense hadron phase. In this simple scenario one assumes that there is no separation of these two phases. The phase transition is terminated when all of the matter is in the hadron phase.

The quantities to be traced through the phase transition are $\epsilon(t)$, $T(t)$, and $R(t)$. These are determined by the equation of state (2.3) and the two Einstein equations

$$\frac{\dot R}{\chi R}=\sqrt{\epsilon/B}, \tag{3.1}$$

$$\frac{3\dot R}{R}=-\frac{\dot\epsilon}{w}, \tag{3.2}$$

where we have used the natural time scale of the problem

$$\chi=\sqrt{8\pi GB/3}=\frac{1}{36\ \mu\text{sec}}\left[\frac{T_c}{200\ \text{MeV}}\right]^2 . \tag{3.3}$$

The solution is given in three pieces, before, during, and after the phase transition.

Before the phase transition, $t < t_i$, the solution is simply given by

$$\left[\frac{T(t)}{T_c}\right]^2 = \frac{\sqrt{(r-1)/3r}}{\sinh 2\chi t}\ , \tag{3.4}$$

$$\frac{R(t)}{R_i} = \frac{T_c}{T(t)}\ . \tag{3.5}$$

This solution is valid until T has decreased to T_c, i.e., until

$$\chi t_i = \tfrac{1}{2}\ln\left[\frac{\sqrt{4r-1}+\sqrt{r-1}}{\sqrt{3r}}\right] = 0.23\ .$$

Numbers here and later are quoted for $r=3$. Note that the effect of the vacuum energy density B to the timing is very small: while the temperature $T_c = 200$ MeV is now [Eq. (3.4)] reached at $t = 8.19$ μsec, the same T without any B would be reached at $t = 8.45$ μsec.

The following stage, during the phase transition, is particularly interesting. The temperature is now constant, $T = T_c$, and also since the pressure is constant, $p = p_c$ the conservation of $S = sR^3$ is equivalent to the conservation of $W = wR^3$. During the phase transition $\epsilon(t)$ decreases from ϵ_Q to ϵ_H [and $s(t)$ from s_Q to s_H, $w(t)$ from w_Q to w_H]. It is convenient to replace $\epsilon(t)$ by $h(t)$, the volume fraction of matter in the hadron phase, by writing

$$\epsilon(t) = \epsilon_H h(t) + \epsilon_Q[1-h(t)]\ . \tag{3.6}$$

The second entropy conservation equation (3.2) can then be written in the form

$$\frac{3\dot{R}}{R} = \frac{\dot{h}}{r/(r-1)-h}\ . \tag{3.7}$$

The two equations (3.1) and (3.7) can now easily be integrated with the result

$$h(t) = 1 - \frac{1}{4(r-1)}\left[\tan^2\left[\arctan\sqrt{4r-1} + \frac{3\chi(t_i-t)}{2\sqrt{r-1}}\right] - 3\right]\ , \tag{3.8}$$

$$\frac{R(t)}{R_i} = (4r)^{1/3}\left[\sin\left[\frac{3\chi(t-t_i)}{2\sqrt{r-1}} + \arcsin\frac{1}{\sqrt{4r}}\right]\right]^{2/3}\ . \tag{3.9}$$

This phase transition stage ends when $h(t)$ has increased to 1. This happens at time

$$\chi t_f = \chi t_i + \tfrac{2}{3}\sqrt{r-1}(\arctan\sqrt{4r-1} - \arctan\sqrt{3}) = \chi t_i + 0.22 = 0.45\ . \tag{3.10}$$

The scale factor $R(t)$ increases to the value

$$R_f = R(t_f) = r^{1/3}R_i\ ,$$

as follows from entropy conservation. Note also that the derivatives of $h(t)$ at the beginning and end are nonzero:

$$\frac{\dot{h}(t_i)}{\chi} = \frac{3r}{r-1}\left[\frac{4r-1}{r-1}\right]^{1/2} = 10.5\ ,$$
$$\frac{\dot{h}(t_f)}{\chi} = \left[\frac{3}{r-1}\right]^{3/2} = 1.84\ . \tag{3.11}$$

The curve $h(t)$ is plotted in Fig. 4.

Finally, after the phase transition for $t > t_f$, we simply have

$$\left[\frac{R(t)}{R_f}\right]^2 = \left[\frac{T_c}{T(t)}\right]^2 = 1 + \left[\frac{12}{r-1}\right]^{1/2}\chi(t-t_f)\ . \tag{3.12}$$

This entirely adiabatic and homogeneous scenario leads to no obvious observable consequences. It is also quite unlikely: usual nucleation theory does not lead to the nonzero derivatives in Eq. (3.11). This simple scenario thus mainly gives us a framework on which to study more realistic and more interesting scenarios.

IV. NUCLEATION OF THE PHASE TRANSITION

In the preceding section, supercooling was entirely neglected. Actually, as the phase transition, by assumption, is of first order, the Universe has to cool somewhat below T_c before any regions of hadron matter can appear. We shall here briefly discuss the nucleation events in a simple thermal nucleation model.[7,8]

Note, first that there are two very different time scales in the problem: the QCD time scale of the order of $1/T_c = 1$ fm and the Hubble time of the order of $1/\chi = 36$ μsec $= 10^{19}/T_c$. We expect that the nucleation is a local phenomenon and knows nothing about the Hubble scale. The rate of bubble nucleation can then be written in the form

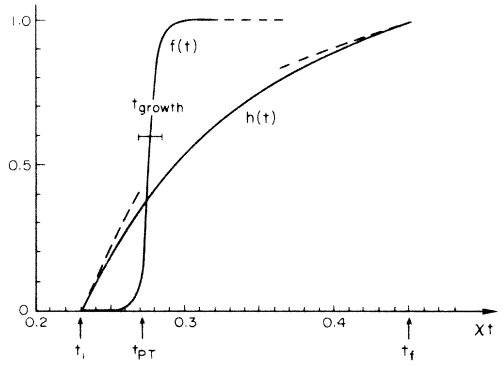

FIG. 4. The volume fraction $h(t)$ of the hadron phase in the no-supercooling scenario and the fraction $f(t)$ of space affected by the nucleated hadron bubbles in the thermal nucleation and supercooling scenario. The function $f(t)$ is plotted schematically; to scale it would be a step function at $t = t_{PT}$ (PT = phase transition). In the small-supercooling—phase-separation scenario it is assumed that $t_{growth} \ll t_{PT} - t_i \ll t_i$.

$$p(t)=p_0 T_c{}^4 \exp\left[-\frac{w_0}{(1-\bar{T}^4)^2}\right], \tag{4.1}$$

where p_0 and w_0 are dimensionless constants, expected to be of the order of 1 and $\bar{T}=T/T_c$. Note that, for $\mu=0$,

$$p_h - p_q = B(1-\bar{T}^4)$$

with the equation of state [(2.1)–(2.4)]. Because of the exponential factor, the rate and all its derivatives vanish at $T=T_c$. For, say, 2% supercooling to $T=0.98T_c$, the exponential factor is $e^{-w_0 165}$. This looks like a small number, but the pre-exponential term $T_c{}^4$, which gives correct dimensions to $p(t)$, is actually large in the Hubble scale: $T_c{}^4 = e^{174}\chi^4$.

After the bubble has been nucleated it grows explosively like a deflagration bubble.[22,23] The structure of these bubbles is shown in Fig. 5. For small few-percent supercoolings, which we shall study here, the phase transition itself propagates rather slowly with a velocity $v_{\rm front} \ll c_s = 1/\sqrt{3}$. This front is preceded by a supersonic shock front moving with velocity $v_{\rm sh} > c_s$ in the quark matter and heating and compressing it.

With increasing time more and more bubbles are nucleated and the bubbles nucleated grow. The fraction of the Universe affected by the shock fronts preceding the growing bubbles is given by

$$f(t) = \int_{t_i}^{t} dt' p(t') \frac{4\pi}{3}[v_{\rm sh}(t'-t_p)]^3 . \tag{4.2}$$

The growth period will be seen to be so brief that the expansion of the Universe can be neglected. Using the equation [see (3.4)]

$$\frac{dT}{T_c} = -\left[\frac{4r-1}{r-1}\right]^{1/2} \chi dt \tag{4.3}$$

we can take scaled T instead of time as variable and calculate the integral by a saddle-point approximation:

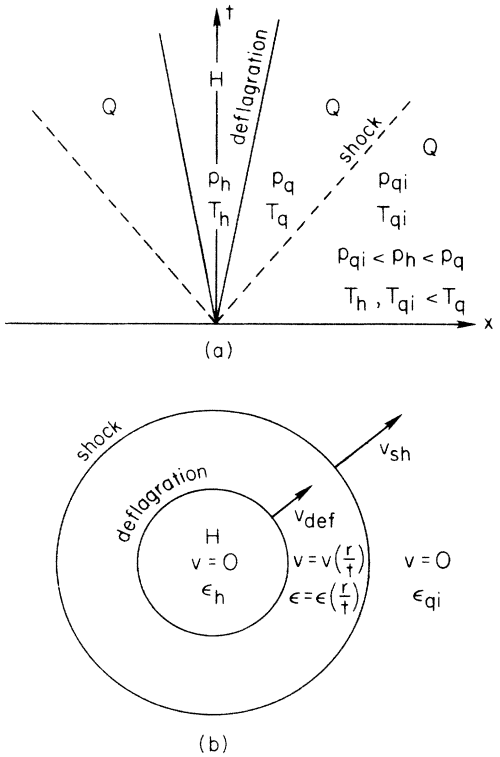

FIG. 5. The structure of a deflagration bubble in (a) 1 + 1 and (b) 1 + 3 dimensions.

$$f(t) = \frac{4\pi}{3} p_0 \frac{T_c{}^4}{\chi^4}\left[\frac{r-1}{4r-1}\right]^2 v_{\rm sh}{}^3 \int_{\bar{T}}^{1} d\bar{T}' \exp\left[-\frac{w_0}{16(1-\bar{T}')^2}\right](\bar{T}'-\bar{T})^3$$
$$= \exp\left[L - \frac{w_0}{16(1-\bar{T})^2} + 12\ln(1-\bar{T})\right], \tag{4.4}$$

where

$$L = \ln[(T_c/\chi)^4 p_0 v_{\rm sh}{}^3] .$$

Since the rate vanishes very rapidly near $T=T_c$, the integrand in (4.4) is very asymmetric and the maximum is very close to the lower limit at

$$\bar{T}' = \bar{T} + \frac{24}{w_0}(1-\bar{T})^3 . \tag{4.5}$$

The behavior of the function $f(t)$ is shown schematically in Fig. 4 together with the fractional amount of hadron matter demanded by the no-supercooling scenario. One sees that the two functions behave very differently. The function $h(t)$ starts growing with a finite derivative. The function $f(t)$ is to begin with essentially zero until it at the time $t=t_{\rm PT}$ suddenly increases to 1. From Eq. (4.4) one sees that $f(t)$ is 1 when T has decreased to

$$T = T_{\rm PT} = [1-(w_0/16L)^{1/2}]T_c = [1-(w_0)^{1/2}/45]T_c \tag{4.6}$$

or at the time [Eq. (4.3)]

$$t_{\rm PT} = t_i + \left[\frac{r-1}{4r-1}\right]^{1/2}\left[\frac{w_0}{16L}\right]^{1/2}\frac{1}{\chi}$$
$$= [0.23 + 0.01(w_0)^{1/2}]/\chi . \tag{4.7}$$

The growth time can be inferred from Eq. (4.5): the bubbles which at $t=t_{\rm PT}$ fill the space were dominantly nucleated at a slightly higher temperature

$$T_{\rm nucl}=T_{\rm PT}+\frac{3}{2L}\left[\frac{w_0}{16L}\right]^{1/2}T_c$$
$$=T_{\rm PT}+\frac{(w_0)^{1/2}}{4800}T_c\ ,$$

so that the growth time is

$$t_{\rm growth}=\frac{3}{2L}\left[\frac{w_0}{16L}\right]^{1/2}\left[\frac{r-1}{4r-1}\right]^{1/2}\frac{1}{\chi}=\frac{W_0}{11\,000}\frac{1}{\chi}\ . \tag{4.8}$$

The initial part of the supercooling scenario thus goes as follows: the Universe comes to $T=T_c$ at $t=t_i$ and initially goes on supercooling in the quark phase. At the time $t=t_{\rm PT}-t_{\rm growth}$ hadron bubbles start being nucleated. More and more bubbles are nucleated and the bubbles grow so that after a period of $t_{\rm growth}$ the shock fronts start colliding. Because $v_{\rm front}\ll v_{\rm sh}$ actually only a small fraction of the matter in the Universe has been converted to the hadron phase. Figuring out what happens next requires new dynamical assumptions about the collisions of bubbles. These will be discussed in the following section: a possible conclusion is that the collisions reheat the quark matter to $T=T_c$ and thus halt the growth of the regions with hadron matter.

An important conclusion of the above is that a new scale appears in the problem.[7] Since the shocked regions grow at the velocity $1/\sqrt{3}$ the average distance between the hadron bubbles is

$$R_i=t_{\rm growth}v_{\rm sh}=(w_0)^{1/2}0.5\ \text{m} \tag{4.9}$$

and the size of the hadron bubbles relative to their separation is $r_i/R_i=v_{\rm front}/v_{\rm sh}\ll 1$. Note that R_i is essentially the Hubble distance 10 780 m divided by the $\frac{3}{2}$ power of the log of the ratio of the fourth powers of the two time scales $1/T_c$ and $1/\chi$ in the problem. R_i is an average distance and there will be lots of small distances as well as a few large distances. The numerical value of R_i is clearly rather badly determined: we shall use as a reference value 1 m.

V. BUBBLE COLLISIONS

After the hadron bubbles have nucleated they grow and the shock fronts preceding the bubbles begin to collide. The Universe enters a turbulent stage, the initial phases of which we shall study in this section. In the small-supercooling case we shall present a scenario, in which this turbulence dies out, the Universe outside the hadron bubbles is reheated to T_c and the explosive bubble growth is halted. Accepting this scenario one can directly continue to Sec. VI, where further expansion-dominated bubble growth is studied.

In this section we will analyze the first collisions between two shock fronts and between a shock and a deflagration front (deflagration + deflagration collisions are rare) in a (1 + 1)-dimensional framework. Since the time scale R_i/c_s is much less than the Hubble time, we ignore the expansion of the Universe. We will first review some general features of the allowed hydrodynamical configurations[29] and then construct specific solutions.[22–24] Most of this section is general and valid for any magnitude of supercooling.

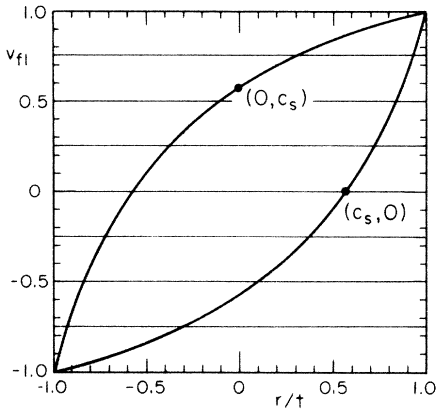

FIG. 6. The two rarefaction-wave solutions $v_{\rm fl}(r/t)$ and a few of the constant solutions of self-similar (1 + 1)-dimensional flow.

Initially there is a configuration of plane shock and deflagration fronts, which separate regions of constant density and flow velocity. Since no length scale comes in, the flow patterns created in collisions of such fronts have a self-similar structure. This means that the density ϵ and flow velocity $v_{\rm fl}$ depend on time and position only through the ratio r/t, where r is the distance from the collision plane and t is the time elapsed since collision. The only allowed flow patterns are then a flow with

$$v_{\rm fl}=\text{const},\quad \epsilon=\text{const}\ , \tag{5.1}$$

and two rarefaction-wave solutions

$$v_{\rm fl}=\frac{r/t\pm c_s}{1\pm c_s r/t},\quad \epsilon=\epsilon(0)\left[\frac{t-r}{t+r}\right]^{\pm(1+c_s^2)/2c_s}\ , \tag{5.2}$$

where $c_s=1/\sqrt{3}$ is the speed of sound and $(1+c_s^2)/2c_s=2/\sqrt{3}$ (see Figs. 6 and 7).

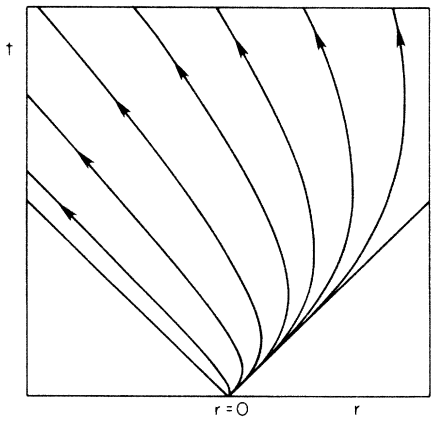

FIG. 7. Flow world lines in a rarefaction-wave solution. This spacetime diagram corresponds to the lower curve in Fig. 6. A corresponding diagram for the upper curve would be a mirror image of this.

Regions of different flow pattern can join at phase boundaries and shock fronts. A rarefaction wave can also change to constant flow at a weak discontinuity front, where only the derivatives of density and flow velocity are discontinuous.

We will now list conditions that must be satisfied at the fronts. We now view the front at its rest frame (Fig. 8). $v_{\rm in}$ and $v_{\rm out}$ are the incoming and outgoing flow velocities in this frame. Later we need these results in a frame where the fluid is at rest on one side of the front. One of these velocities becomes then the front velocity and we get the flow velocity on the other side by boosting the other velocity by this one.

Energy and momentum conservation relate the velocities $v_{\rm in}$ and $v_{\rm out}$ by

$$v_{\rm in}v_{\rm out}=\frac{p_{\rm in}-p_{\rm out}}{\epsilon_{\rm in}-\epsilon_{\rm out}},\quad \frac{v_{\rm out}}{v_{\rm in}}=\frac{\epsilon_{\rm in}+p_{\rm out}}{\epsilon_{\rm out}+p_{\rm in}} \tag{5.3}$$

(Ref. 30). Using $p=\frac{1}{3}\epsilon$ in H phase and $p=\frac{1}{3}(\epsilon-4B)$ in Q phase we get for a shock front

$$v_{\rm in}v_{\rm out}=c_s{}^2 . \tag{5.4}$$

If the shock front is in the Q region

$$\frac{v_{\rm out}}{v_{\rm in}}=\frac{3\epsilon_{\rm in}+\epsilon_{\rm out}-4B}{\epsilon_{\rm in}+3\epsilon_{\rm out}-4B} , \tag{5.5}$$

and if it is in the H region

$$\frac{v_{\rm out}}{v_{\rm in}}=\frac{3\epsilon_{\rm in}+\epsilon_{\rm out}}{\epsilon_{\rm in}+3\epsilon_{\rm out}} . \tag{5.6}$$

For a phase transition front (incoming flow in Q phase, outgoing in H phase)

$$\frac{v_{\rm out}}{v_{\rm in}}=\frac{3\epsilon_{\rm in}+\epsilon_{\rm out}}{\epsilon_{\rm in}+3\epsilon_{\rm out}-4B} \tag{5.7}$$

and

$$v_{\rm in}v_{\rm out}=\frac{1}{3}\frac{\epsilon_{\rm out}-\epsilon_{\rm in}+4B}{\epsilon_{\rm out}-\epsilon_{\rm in}}>c_s{}^2 \tag{5.8}$$

for a detonation ($v_{\rm in}>v_{\rm out}$) case, and

$$v_{\rm in}v_{\rm out}=\frac{1}{3}\frac{\epsilon_{\rm in}-\epsilon_{\rm out}-4B}{\epsilon_{\rm in}-\epsilon_{\rm out}}<c_s{}^2 \tag{5.9}$$

for a deflagration ($v_{\rm out}>v_{\rm in}$) case. Since a detonation requires that the H phase has a much higher density than the Q phase, $\epsilon_{\rm out}\geq\epsilon_{\rm in}+2B$ (otherwise $v_{\rm in}v_{\rm out}>1$) it is unlikely that detonation fronts occur. A deflagration requires $\epsilon_{\rm in}\geq\epsilon_{\rm out}+4B$, a more likely circumstance. Yet another possibility is a contact surface, where both phases are under the same pressure, i.e.,

$$\epsilon_{\rm out}=\epsilon_{\rm in}-4B \tag{5.10}$$

and

$$v_{\rm in}=v_{\rm out}=0 . \tag{5.11}$$

In a phase transition there is a change of total entropy. The condition of non-negative entropy production is

$$\frac{\epsilon_{\rm out}}{\epsilon_{\rm in}-B}\geq r\frac{(\epsilon_{\rm in}+3\epsilon_{\rm out}-4B)^2}{(3\epsilon_{\rm in}+\epsilon_{\rm out})^2} . \tag{5.12}$$

From Eqs. (5.4)–(5.9) it follows that $v_{\rm out}=c_s$ is possible for the phase transition fronts but not for a shock front, and that $v_{\rm in}=c_s$ is not possible. This is important because of a special feature of the rarefaction waves [Eq. (5.2)]. Let there be a self-similar flow pattern where a region of rarefaction flow ends at a (shock or phase transition) front. At time t the front will be located at $r=v_{\rm front}t$. From Eq. (5.2) we see that the flow velocity in the rarefaction wave is $v_{\rm fl}=(v_{\rm front}\pm c_s)/(1\pm c_s v_{\rm front})$ here. Boosting with $v_{\rm front}$ to the front frame we obtain

$$v_{\rm in\,(out)}=c_s$$

for an incoming (outgoing) rarefaction wave.

The conclusion is that rarefaction waves in the H phase may border to deflagration or detonation fronts, but rarefaction waves in the Q phase must have a weak discontinuity on both sides. Since the rarefaction wave carries with it information on the distance from its origin, the flow pattern resulting from a collision with a rarefaction wave is not self-similar anymore. We shall not pursue these more complicated patterns here.

Aided with the preceding guidelines we now proceed to construct some possible configurations. We begin with an idealized initial situation of equidistance narrow H regions ("bubbles") all nucleated at the same moment t_0. The first event is a collision of two shock fronts. With the notation of Fig. 9 we have the conditions

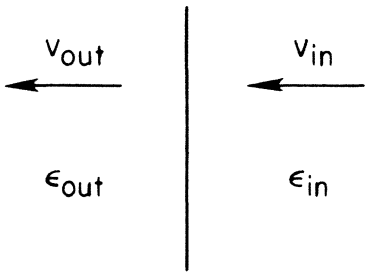

FIG. 8. A front viewed in its rest frame. For a shock front, both the incoming and outgoing flow are in the same phase, while for a phase transition front the incoming flow is in the Q phase and the outgoing in the H phase.

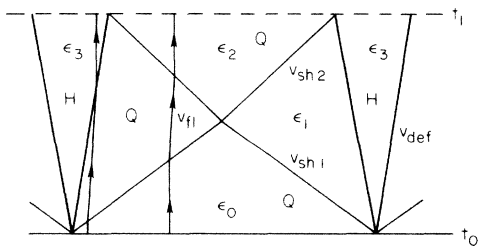

FIG. 9. A spacetime diagram of the first stage of our (1 + 1)-dimensional scenarios. The deflagration bubbles grow with velocity $v_{\rm def}$ until their surfaces collide with the reflected shock fronts. The shocks heat the Q phase from ϵ_0 to ϵ_2 (from $T_{\rm PT}<T_c$ to a temperature above or below T_c).

$$v_{\rm def}{}^2=\frac{1}{3}\frac{(3\epsilon_1+\epsilon_3)(\epsilon_1-\epsilon_3-4B)}{(\epsilon_1-\epsilon_3)(3\epsilon_3+\epsilon_1-4B)}\ , \tag{5.13}$$

$$\begin{aligned} v_{\rm fl}{}^2&=3\frac{(\epsilon_1-\epsilon_3)(\epsilon_1-\epsilon_3-4B)}{(3\epsilon_1+\epsilon_3)(\epsilon_1+3\epsilon_3-4B)}\\ &=3\frac{(\epsilon_1-\epsilon_0)^2}{(3\epsilon_1+\epsilon_0-4B)(\epsilon_1+3\epsilon_0-4B)}\\ &=3\frac{(\epsilon_2-\epsilon_1)^2}{(3\epsilon_2+\epsilon_1-4B)(\epsilon_2+3\epsilon_1-4B)}\ , \end{aligned} \tag{5.14}$$

$$v_{\rm sh1}{}^2=\frac{1}{3}\frac{3\epsilon_1+\epsilon_0-4B}{\epsilon_1+3\epsilon_0-4B}\ , \tag{5.15}$$

$$v_{\rm sh2}{}^2=\frac{1}{3}\frac{3\epsilon_1+\epsilon_2-4B}{\epsilon_1+3\epsilon_2-4B}\ . \tag{5.16}$$

To solve the eight quantities from these six equations we need to specify two of the quantities. Since the propagation velocity of the deflagration front depends on the unknown microphysics within the front, we are not able to uniquely determine the quantities from the initial condition

$$\epsilon_0=g_q\frac{\pi^2}{30}T_{\rm PT}{}^4=\frac{4r-1}{r-1}B\left[\frac{T_{\rm PT}}{T_c}\right]^4, \tag{5.17}$$

but are left with one unknown parameter, which we can take to be, e.g., ϵ_3 or $v_{\rm def}$. Its allowed range is, however, restricted by the entropy condition

$$\frac{\epsilon_3}{\epsilon_1-B}\geq r\left[\frac{3\epsilon_3+\epsilon_1-4B}{3\epsilon_3+\epsilon_1}\right]^2. \tag{5.18}$$

The possible region in the (ϵ_3,ϵ_1) plane is restricted by $\epsilon_1>\epsilon_3+4B$ and Eq. (5.18). We use Eq. (5.14) to map this region onto the (ϵ_3,ϵ_0) and (ϵ_3,ϵ_2) planes (Fig. 10). We see that the density of the H bubble is restricted by

$$\epsilon_3>\epsilon_0-4B \tag{5.19}$$

from below and by the entropy condition from above. The H phase can be hotter or colder than the unshocked Q region (with temperature $T_{\rm PT}<T_c$), but it is always colder than the shocked Q region and below T_c.

From the last equality of Eq. (5.14) follows

$$\frac{\epsilon_2-B}{\epsilon_1-B}=\frac{\epsilon_1-B}{\epsilon_0-B}\ . \tag{5.20}$$

Substituting this into Eqs. (5.15) and (5.16) gives

$$v_{\rm sh1}v_{\rm sh2}=\tfrac{1}{3}=c_s{}^2\ . \tag{5.21}$$

Since a shock always propagates faster than sound into a medium at rest, we have

$$v_{\rm sh2}<c_s<v_{\rm sh1}\ . \tag{5.22}$$

Thus the first shock heats the Q region from $\epsilon_0<\epsilon_3+4B$ (below T_c) to $\epsilon_1>\epsilon_3+4B$ (above or below T_c) and the reflected shock further heats it to ϵ_2 (above or below T_c).

Figure 10 is general and applies for arbitrarily large supercoolings. The small-supercooling scenario needs only the region very close to the point ϵ_Q,ϵ_H. As a concrete example, let us approach this point along the $\Delta S=0$ curve [equality sign in Eq. (5.18)]. In the limit of small supercooling $\Delta T=T_c-T_{\rm PT}\ll T_c$ we then have[23]

$$v_{\rm def}=\frac{4r-1}{\sqrt{3}(r-1)}\frac{\Delta T}{T_c},\quad v_{\rm fl}=\frac{4r-1}{\sqrt{3}r}\frac{\Delta T}{T_c}\ . \tag{5.23}$$

The temperatures of the four regions are then

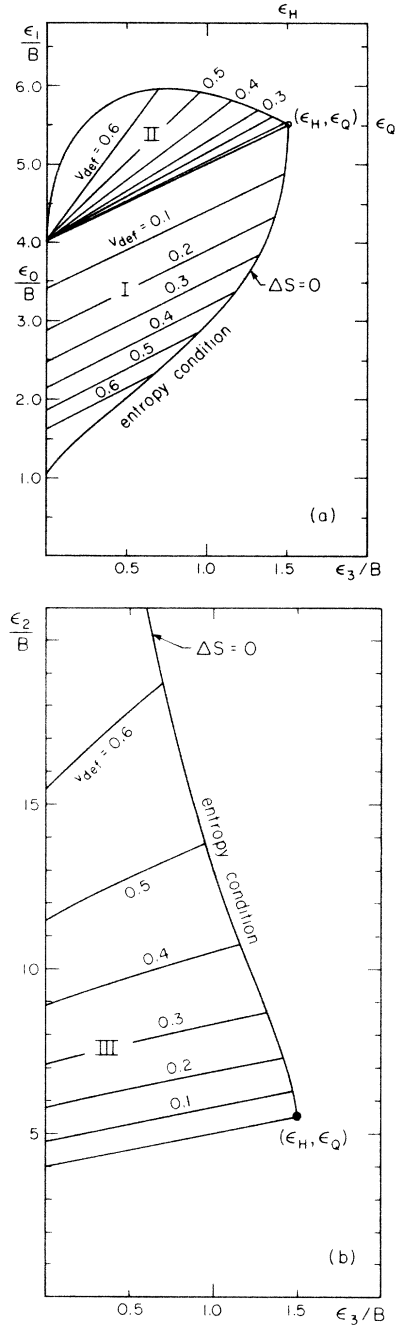

FIG. 10. (a) and (b) show the allowed energy density combinations for the process of Fig. 9. For a given initial Q density ϵ_0 there is a range of possible H densities ϵ_3 and corresponding deflagration velocities $v_{\rm def}$ represented by region I. Regions II and III give the corresponding Q densities ϵ_1 (shocked once) and ϵ_2 (shocked twice).

$$T_0=T_c-\Delta T\ ,$$
$$T_1=T_c+\frac{(4r-1)^2}{6r(r-1)}\frac{\Delta T}{T_c}\Delta T\approx T_c\ ,$$
$$T_2=T_c+\Delta T\ ,$$
$$T_3=T_c-\frac{(4r-1)^2}{6r(r-1)}\frac{\Delta T}{T_c}\Delta T\approx T_c\ , \tag{5.24}$$

and the shock velocities are

$$v_{\rm sh1}=c_s\left[1+\frac{4r-1}{3r}\frac{\Delta T}{T_c}\right]\ ,$$
$$v_{\rm sh2}=c_s\left[1-\frac{4r-1}{3r}\frac{\Delta T}{T_c}\right]\ . \tag{5.25}$$

In our symmetric idealization all of the matter is momentarily at rest at time t_1 when the reflected shock front collides with the phase boundary. The space is now divided into narrow H and wide Q regions. Since the shocks heated the Q phase to $\epsilon_2>\epsilon_3+4B$, the deflagration front can no longer propagate in the same way as before t_1. Depending on the values ϵ_2,ϵ_3 there are several possibilities as to what happens in this collision.

One possibility [process (a) of Fig. 11] is that a somewhat different deflagration configuration arises, resembling the surface deflagration in Ref. 22. Here the reflected shock front penetrates into the H phase. The flow velocity $v_{\rm fl2}$ is related to the densities by

$$v_{\rm fl}{}^2=\frac{3(\epsilon_2-\epsilon_4)(\epsilon_2-\epsilon_4-4B)}{(3\epsilon_2+\epsilon_4)(\epsilon_2+3\epsilon_4-4B)}$$
$$=\frac{3(\epsilon_4-\epsilon_3)^2}{(3\epsilon_4+\epsilon_3)(\epsilon_4+3\epsilon_3)}$$
$$=\frac{3(\epsilon_5-\epsilon_4)^2}{(3\epsilon_5+\epsilon_4)(\epsilon_5+3\epsilon_4)}\ , \tag{5.26}$$

and from this we can solve

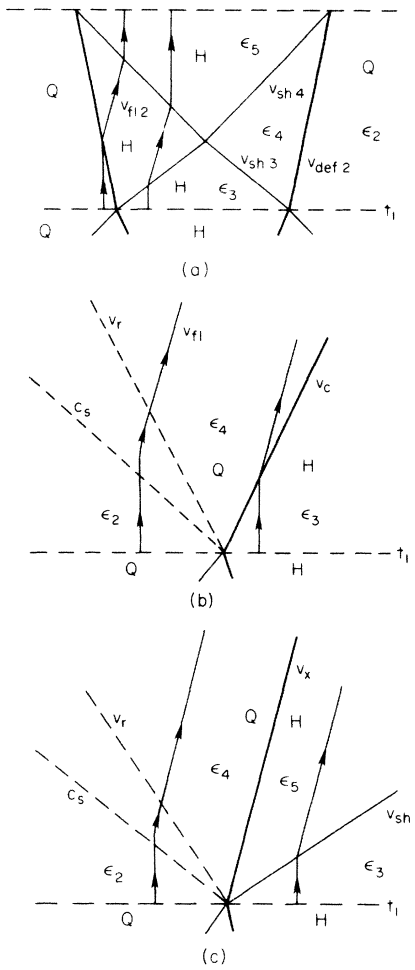

FIG. 11. Spacetime diagrams for three different processes that can follow after the matter has been momentarily brought to rest at $t=t_1$. (a) The reflected shock fronts penetrate the H region, heating it up. The deflagration front is slowed down, but proceeds further into the Q phase. (b) The direction of the phase transition is reversed and a compression front begins to eat up the H region. The produced Q matter follows the compression front leaving a rarefaction wave behind. (c) The phase transition may halt. The phase boundary then becomes a contact surface parallel to H and Q flow world lines. This requires that H and Q be brought to the same pressure, H pressure raised by a shock and Q pressure reduced by a rarefaction wave. Particle paths are denoted by lines with arrows.

$$\epsilon_4=\frac{\epsilon_3B+\{\epsilon_3{}^2B^2+[(\epsilon_2-B)-\epsilon_3][\epsilon_2(\epsilon_2-4B)\epsilon_3-(\epsilon_2-B)\epsilon_3{}^2]\}^{1/2}}{\epsilon_2-\epsilon_3-B}\ , \tag{5.27}$$

$$\epsilon_5=\frac{\epsilon_4{}^2}{\epsilon_3}\ . \tag{5.28}$$

The deflagration front gives again an entropy condition

$$\frac{\epsilon_4}{\epsilon_2-B}\geq r\frac{(3\epsilon_4+\epsilon_2-4B)^2}{(3\epsilon_2+\epsilon_4)^2}\ . \tag{5.29}$$

The allowed region in the (ϵ_4,ϵ_2) plane is the same as region II of Fig. 10 in the (ϵ_3,ϵ_2) plane. Mapping this region on to the (ϵ_3,ϵ_2) plane, we see that this process is allowed only in the case of a rather moderate heating of the Q phase corresponding to the slowest deflagrations.

If the Q phase has become too hot to allow deflagration, we might expect that the direction of the phase transition be reversed. Figure 11(b) shows this kind of compressive transition of H matter into Q matter.

Since the H phase is at lower density, a shrinking H phase cannot maintain the density of the Q phase. Therefore a rarefaction wave forms here. The quantities on both sides of the rarefaction wave are related by

$$\epsilon_4 - B = (\epsilon_2 - B)\left[\frac{1+v_{\rm fl}}{1-v_{\rm fl}}\right]^{-2/\sqrt{3}}, \tag{5.30}$$

where

$$v_{\rm fl} = \frac{v_r + c_s}{1 + v_r c_s}. \tag{5.31}$$

Figure 12 shows the region allowed by the entropy condition

$$\frac{\epsilon_3}{\epsilon_4 - B} = r\frac{(3\epsilon_3 + \epsilon_4 - 4B)^2}{(3\epsilon_4 + \epsilon_3)^2}. \tag{5.32}$$

There is a third kind of process possible, not restricted by an entropy condition. This is a configuration, where the Q and H phases have equal pressure and flow parallel to a contact surface between them. A rarefaction wave is needed here to lower the Q pressure. As the Q matter is blown outwards from the rarefaction wave, the contact surface is pushed towards the H phase, creating a shock there [see Fig. 11(c)]. In most cases the further evolution

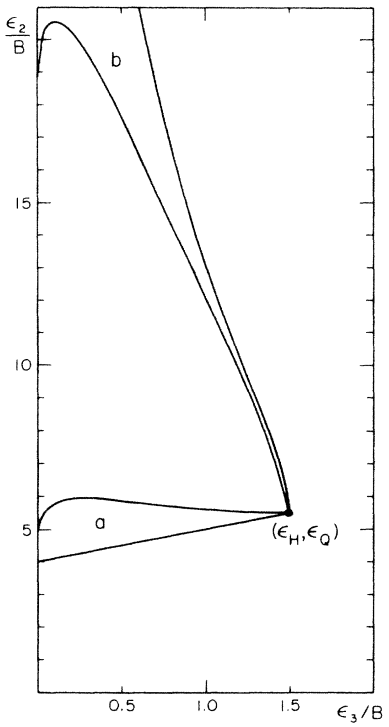

FIG. 12. The first two processes [(a) and (b)] of the configurations in Fig. 11 are restricted by an entropy condition for the phase transition front. Thus, they are not possible for all values (ϵ_2, ϵ_3) that may be produced in the first stage (region III of Fig. 10), but only for certain parts [(a) and (b)] of this region. Process (a) is allowed only if the deflagration front of the first stage chose to proceed slowly leaving the H matter close to the minimum allowed density. Process (b) is allowed close to the $\Delta S = 0$ curve.

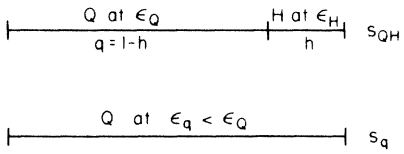

FIG. 13. The entropy of supercooled Q matter (bottom line) is lower than that of the maximum-entropy state (top line) where the same energy is distributed to H and Q regions at the critical temperature. h and q are the required volume fractions of the two phases.

becomes intractable after a few collision periods. The direction of entropy growth, however, points towards the state of maximum entropy, where the matter has settled down to coexisting Q and H phases, reheated to the critical temperature (Fig. 13). Supercooled Q matter at $T_{\rm PT} < T_c$ has an entropy density

$$s_q = g_q\left[\frac{4\pi^2}{90}\right]T_{\rm PT}{}^3, \tag{5.33}$$

while the average entropy density for the coexisting phases is

$$s_{QH} = [hg_h + (1-h)g_q]\left[\frac{4\pi^2}{90}\right]T_c{}^3, \tag{5.34}$$

where h is the H volume fraction. If we assume that this state is reached fast enough to let us ignore expansion, h can be solved from energy conservation:

$$h = \frac{3}{4}\frac{r}{r-1}\left[1 - \left[\frac{T_{\rm PT}}{T_c}\right]^4\right] \tag{5.35}$$

and the entropy production is then

$$s_{QH} - s_q = (\tfrac{3}{2}\delta^2 - 2\delta^3 + \tfrac{3}{4}\delta^4)g_q\left[\frac{4\pi^2}{90}\right]T_c{}^3, \tag{5.36}$$

where $\delta = (T_c - T_{\rm PT})/T_c$ (see Fig. 14).

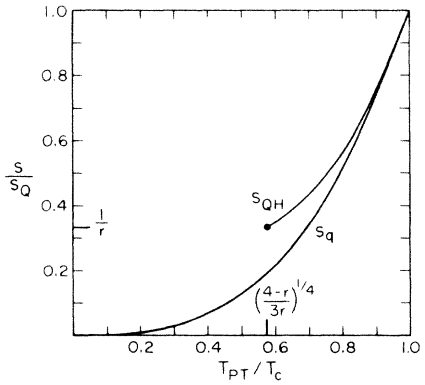

FIG. 14. The entropy densities of the two states of Fig. 13 as a function of the temperature of the supercooled Q matter. $[(4-r)/3r]^{1/4}T_c$ is the lowest temperature (corresponding to total conversion to H phase) from which the phase transition can reheat matter to the critical temperature.

Actually the expansion will maintain a small temperature difference

$$\Delta T/T_c \sim (\chi R)^2 \tag{5.37}$$

between coexisting phases of size $\sim R$. The question is whether the temperatures are brought within this distance of T_c in a time less than the phase transition time $\sim 0.22/\chi$. If they are, then the latter part of the phase transition era will proceed peacefully as described in Secs. VI–IX.

There is one scenario which is easy to follow. Assume the initial deflagration velocity is very small. In the (ϵ_q, ϵ_h) plane we are then very close to the equal pressure line $\epsilon_q = \epsilon_h + 4B$. Because of the small velocities this is a case with very low entropy production, even though we are farthest (for a given ϵ_q) from the line $\Delta S = 0$. The deflagration process then remains allowed even after repeated reheating by shocks. The bubble growth would then proceed as shown in Fig. 15. As weak shocks pass through the Q and H regions, these are gradually reheated towards T_c (see Fig. 16). When either region is finally heated above T_c, this will give way to some other process; to make an estimate, assume, however, this takes almost all of the phase transition time. In that case $\Delta T \equiv T_c - T$ is reduced by a factor $\sim \chi R_i$. Since from Sec. II we have that R_i and $\Delta T_1 \equiv T_c - T_{\rm PT}$ are related by $\Delta T_1/T_c \sim R_i/20$ m $\sim 10^3 \chi R_i$, we are still a factor of 10^3 away from the criterion (5.37).

Since we intentionally chose a case with a very low entropy production rate, this is more like a worst-case scenario, and we cannot conclude that T_c would not be attainable with accuracy (5.37) in general. Note that the factor 10^3 above was independent of R_i, although the final ΔT was proportional to ${R_i}^2$. This is because our criterion was also $\sim R^2$, and we assumed $R \sim R_i$. In the case that the initial bubbles are fairly small ($\sim$centimeter or less) they will during the phase transition coalesce to larger ($\sim$1–10 cm) bubbles,[9] which will make the criterion (5.37) easier.

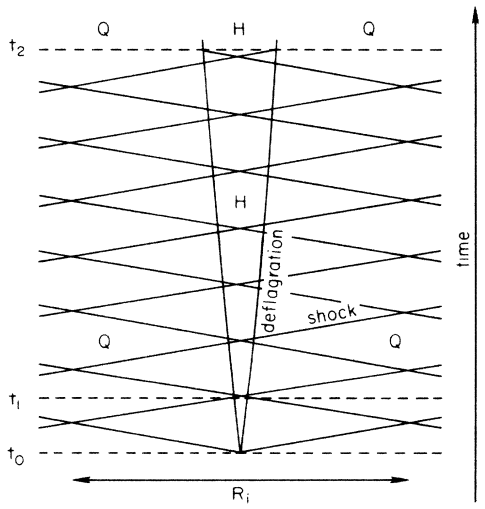

FIG. 15. In the slow-deflagration scenario shocks gradually reheat both the Q and H phases, until at time t_2, one of them is heated above T_c. This figure is for $R_i = 1$ m, $T_{\rm PT} = 0.96 T_c$, and $v_{\rm def} = 0.01$, which gives $t_2 - t_0 = 40$ nsec.

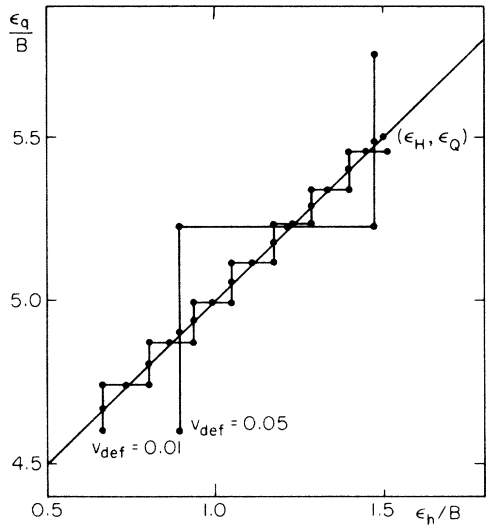

FIG. 16. The process of Fig. 15 in the (ϵ_h, ϵ_q) plane. The shocks first raise twice the density of the Q phase, then twice the H phase, and so on. For comparison we show also a process with a 5 times faster deflagration. T_c is reached now much faster but less accurately

The methods of this section can also be applied to the problem of a dying Q droplet. Assume a situation like the one we have at $t = t_1$ of Figs. 9 and 11, but instead of the Q regions being wide and the H regions narrow, let us study the opposite situation. The slow-deflagration scenario [process (a)] would then proceed as shown in Fig. 17. When not disturbed by reflected shock waves, the deflagration fronts would finally meet, eliminating the Q phase. Because of the outward flow, a rarefaction wave forms as the source supplying this flow has vanished. The final rarefied density ϵ_5 is very close to the initial unshocked density ϵ_3 [they are equal to second order in $(\epsilon_4 - \epsilon_3)/\epsilon_3$]. The rarefaction wave will finally catch up with the shock wave and reflect from it, slowing down

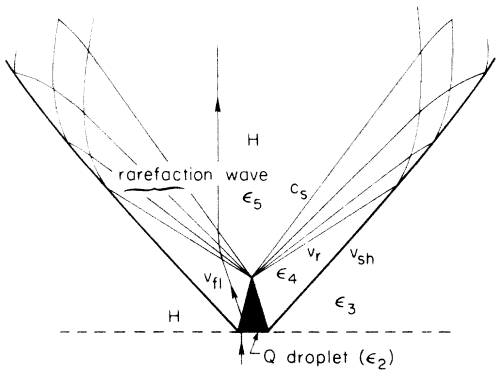

FIG. 17. A dying 1D Q droplet.

and weakening the shock front. Quantitative analysis can be performed as above.

It is clear that a detailed analysis of the initial shock-wave collision stage is extremely complex, especially in three dimensions and for deep supercoolings, and above we have just studied a few important initial processes. It has not been possible to prove that the temperature will rise back to T_c and halt for the moment further expansion. However, this is still quite plausible and we shall proceed to study further expansion-dominated bubble expansion in the following section.

VI. THE SMALL-SUPERCOOLING–PHASE-SEPARATION SCENARIO

After the events described in the two preceding sections, the Universe is in a state containing mainly leptons, neutrinos, and quark-gluon matter at the temperature $T=T_c$. In addition, there are small bubbles of hadron matter of average size r_i and at an average distance R_i ($r_i/R_i=v_{\rm def}/c_s \ll 1$). The whole duration of this initial period, as computed above in Eq. (4.7), is much less than the total duration $0.22/\chi$ of the phase transition period, if the initial supercooling is small (the parameter w_0 is small). We shall now assume that this is the case.

If the initial supercooling is large, the shock-front collision stage described in Sec. V will last over the entire phase transition period. This very turbulent scenario[7–9] will not be discussed further in this paper, although it may lead to potentially very interesting phenomena like black-hole formation or gravitational radiation.

To describe the further sequence of events we shall also first use a (1 + 1)-dimensional approximation, i.e., assume that the bubbles are rather slabs. This greatly simplifies the discussion of the essential points, transport of entropy, and baryon number. With the intuition gained by this simplification, it is easier to discuss the physical (1 + 3)-dimensional case (Sec. IX).

In this scenario the later history of the phase transition is as shown in Fig. 18. From t_i on the Universe goes on expanding and the increase in volume is filled by converting matter from the denser quark phase to the less-dense hadron phase. The hadron bubbles grow until all the Universe is filled by hadron matter at $t=t_f$. The most essential difference between this scenario and the scenario in Sec. III is thus that the phases are entirely separated. Note also that with the linear scale of Fig. 18 all the complex events of Secs. IV–V take place within the line $t=t_i$. It is thus very singular. Some remnant of the turbulence of this initial period may persist to μsec time scale to disturb the expansion dominated behavior shown here.

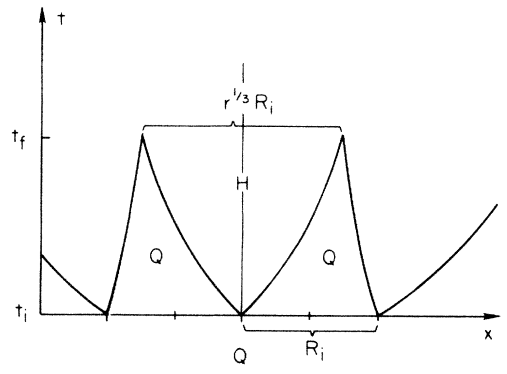

FIG. 18. The sequence of events in the small-supercooling–phase-separation scenario. Initial bubble nucleations and shock front collisions take place within the singular line $t=t_i$.

A very similar model for the phase transition in nucleus-nucleus collisions has been proposed by Van Hove.[25] Models for nucleus-nucleus collisions corresponding to the scenario in Sec. III have been discussed in Refs. 17–23. In these cases the system is actually much more complicated since it is both inhomogeneous and nonisotropic.

Consider then more quantitatively how the conservation of entropy constrains bubble growth. Baryon number will be neglected here and discussed in Sec. VIII. Since $T=T_c$ the entropy densities of the Q and H regions in Fig. 18 are s_Q and s_H. Since $p=p_c$ and $w=\epsilon+p_c+T_c s$ we can as well use the enthalpy density w. The total enthalpies in a region of radius $R(t)$ are then

$$W_h=w_H h(t)R(t)^3,\quad W_q=w_Q[1-h(t)]R(t)^3\ , \tag{6.1}$$

where $h(t)$ is the volume fraction of hadron matter. The conservation of total entropy implies that $\dot{W}=\dot{W}_h+\dot{W}_q=0$ or that

$$\dot{W}_h=w_H R^3\left[\dot{h}+h\frac{3\dot{R}}{R}\right]=-\dot{W}_q=w_Q R^3\left[\dot{h}-(1-h)\frac{3\dot{R}}{R}\right]. \tag{6.2}$$

Since $w_Q/w_H=r$ this is just Eq. (3.7). In the (1 + 1)D approximation, entropy conservation then means that there must be a flux of enthalpy across the wall from the Q to the H regions determined by

$$2F_w R^2=\dot{W}_h\ .$$

This gives the required enthalpy flux

$$F_w(t)=w_H\frac{3r}{2(r-1)}\dot{R}(t)\ , \tag{6.3}$$

the entropy flux is simply $F_s=F_w/T_c$. $F_w(t)$ can thus be computed from $R(t)$ in Eq. (3.9).

Given $R(t)$ and $h(t)$ we can also compute the velocity v_F and path of the bubble walls in Fig. 18. In the (1 + 1)D approximation we simply have

$$h(t)=2\int_{t_i}^{t}\frac{dt'}{R(t')}v_F(t')\ , \tag{6.4}$$

from which

$$v_F(t)=\tfrac{1}{2}R(t)\dot{h}(t)\ . \tag{6.5}$$

We shall from now on normalize the curvature parameter $R(t)$ so that $R(t_i)=R_i$, the average distance between the hadron bubbles at the start of the growth period. The growth of a single bubble is then shown in Fig. 19 and the variation of the wall velocity v_F in Fig. 20. As concerns the magnitudes, they are essentially determined by χR_i,

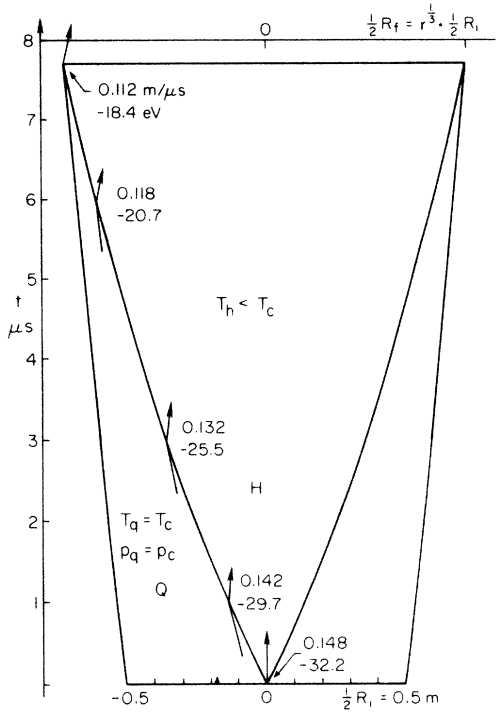

FIG. 19. Details of the growth of a single hadron bubble in the (1 + 1)-dimensional approximation. The scales in the time and space directions are approximately 1:10000 and 1:10. The arrows show the directions of matter flow and the numbers show the magnitude of the velocity and the difference $T_h - T_c$.

i.e., the ratio of the initial bubble distance and the Hubble distance. We can, namely, from Eq. (3.9) compute

$$\dot{R}(t_i) = \left[\frac{4r-1}{r-1}\right]^{1/2} \chi R_i \ ,$$
$$\dot{R}(t_f) = \left[\frac{3}{r-1}\right]^{1/2} \chi R_i \ . \tag{6.6}$$

The magnitude of F_w thus essentially is $w_H \chi R_i$. Similarly, from Eq. (3.11) the magnitude of v_F varies between the limits

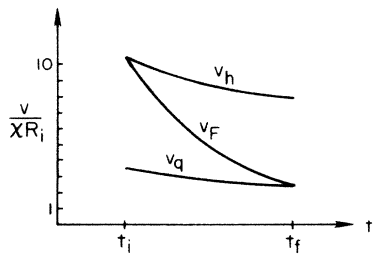

FIG. 20. The variation of the bubble wall velocity v_F and the matter velocities into the front from the Q phase (v_q) and from the front into the hadron phase (v_h) in the rest frame of the front. Note that $v_h = 3v_q$ from entropy conservation: the matter takes more space in the hadron phase.

$$\left[\frac{3}{2(r-1)}\right]^{3/2} r^{1/3} < \frac{v_F}{\chi R_i} < \frac{3r}{2(r-1)} \left[\frac{4r-1}{r-1}\right]^{1/2} . \tag{6.7}$$

Increasing the amount of initial supercooling increases the initial R_i and, consequently, the required entropy flux and the bubble wall velocity. Conversely, with less and less supercooling the bubbles get smaller and smaller and one approaches the homogeneous no-phase-separation scenario of Sec. III.

With the total flux required now determined, the next question is what causes this flux. As pointed out by Witten,[9] there are two types of flux: a hydrodynamic flux $F_{\rm hd}$ with matter transfer and a radiative flux $F_{\rm rad}$ carried by neutrinos, electrons, and photons. Their expected relative amount has been studied by Applegate and Hogan.[12] In the following section we shall study the consequence of a purely hydrodynamic entropy transfer.

VII. PHASE-SEPARATION SCENARIO WITH HYDRODYNAMIC MATTER TRANSFER

In this scenario the matter is converted from the Q to the H phase across a singular deflagration front over which the thermodynamic and flow quantities change discontinuously. In the rest frame of the front and for $v \ll 1$ the standard continuity equations of energy and momentum flux and of baryon number (included here for use in Sec. VIII) are

$$F_{hd} = w_H v_h = w_Q v_q \ ,$$
$$w_H v_h^{\,2} + p_h = w_Q v_q^{\,2} + p_q \ , \tag{7.1}$$
$$n_h v_h = n_q v_q \ .$$

Solving for F_{hd} and using

$$p_q = p_c, \quad p_c - p_h = w_H \left[1 - \frac{T_h}{T_c}\right] ,$$

one has

$$F_{hd} = w_H \left[\frac{r}{r-1}\right]^{1/2} \left[\frac{T_c - T_h}{T_c}\right]^{1/2} . \tag{7.2}$$

We now assume that all the enthalpy flux required by the adiabatic expansion of the Universe and given in Eq. (6.3), is caused by hydrodynamic matter transfer. Then $F_{hd} = F_w$ and Eqs. (6.3) and (7.1) and (7.2) give that

$$v_q = \frac{3}{2(r-1)} \dot{R}(t) \ ,$$
$$v_h = \frac{3r}{2(r-1)} \dot{R}(t) = r v_h \ , \tag{7.3}$$
$$\frac{T_c - T_h}{T_c} = \frac{9r}{4(r-1)} \dot{R}(t)^2 \ .$$

These quantities are shown in Figs. 19 and 20. Again the velocities are of the order of $\chi R_i (= 10^{-4}$ for the reference value $R_i = 1$ m) and the temperature of the hadron matter is required to be less than T_c by an amount $(\chi R_i)^2 T_c =$ the order of 10 eV. For the change in the

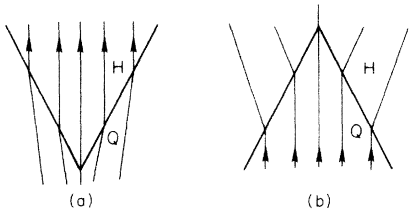

FIG. 21. The flow patterns (a) near the birth of a hadron bubble and (b) near the death of a quark droplet. The patterns are singular at the beginning and the end.

baryon-number density one similarly obtains

$$\frac{n_q}{n_h}=r \tag{7.4}$$

and the baryon-number flux across the front is

$$j_b=2R^2 n_q v_q=2R^2 n_h v_h \ ,$$

where n_q is the tiny initial cosmological baryon-number density ($n_c/s_Q=10^{-9}$) and v_h and v_q are given in (7.3).

Consider then the initial and final values of the different velocities. From the above equations we directly obtain

$$\begin{aligned} v_F(t_i)=v_h(t_i)&=\frac{3r}{2(r-1)}\left[\frac{4r-1}{r-1}\right]^{1/2}\chi R_i \ , \\ v_F(t_f)=v_q(t_f)&=\frac{1}{2}\left[\frac{3}{r-1}\right]^{3/2}\chi R_i \ . \end{aligned} \tag{7.5}$$

If we now Lorentz transform from the rest frame of the front to the frame in which v_F has the appropriate value, the first of Eqs. (7.5) implies that v_h is transformed to zero and the second that v_q is transformed to zero. Initially matter inside the H bubble is at rest, while at the end matter in the Q droplets is at rest. The situation is thus as shown in Fig. 21. The pattern is clearly singular at the end and at the beginning. The required flow pattern at the beginning has to be created by the complex bubble nucleation and shock-front collision events discussed in Secs. IV and V. At the end the outward ejection of hadron matter from the quark droplet will lead to inhomogeneities in the matter distribution of the Universe, which we estimate next.

After the quark droplet has decayed the flow pattern will still persist for some time further away. Since this pattern was keeping the density of the H region constant, parts of the Universe will stay at density $\epsilon_n \approx \epsilon_H$ until a rarefaction wave from the droplet death arrives. Since this flow is carrying matter away from where the droplet was, a region of lower density forms there.

Looking closely at the droplet decay site (Fig. 22) the expansion of the Universe can be ignored for a short time. We then have the dying droplet case of Sec. V. Possible effects from the baryon number are ignored here (see Sec. VIII). Hadronic matter is flowing away with the velocity

$$v_{\rm fl}=(r-1)v_F=\frac{3}{2}\left[\frac{3}{r-1}\right]^{1/2}\chi R_i$$

(clearly nonrelativistic) leaving behind a region at lower density

$$\begin{aligned} \epsilon_r&=\epsilon_h \exp\left[-\frac{1+c_s^2}{c_s}\operatorname{arctanh} v_{\rm fl}\right] \\ &\approx \epsilon_H\left[1-\frac{6}{\sqrt{r-1}}\chi R_i\right] . \end{aligned}$$

This region expands at the speed of sound $c_s=1/\sqrt{3}$. Between the regions of high (ϵ_H) and low (ϵ_r) density there is a rarefaction wave, the front of which has the velocity

$$v_r=\frac{c_s+v_{\rm fl}}{1+c_s v_{\rm fl}}\approx c_s+\left[\frac{3}{r-1}\right]^{1/2}\chi R_i \ .$$

Farther away the flow will be slower (since the H fluid is at rest halfway between droplets). It is just this velocity gradient that keeps ϵ_h constant in the presence of expansion. As the rarefaction wave proceeds into these regions, it gets narrower and the density drop across it becomes smaller, until it disappears half-way (Fig. 23). The time taken by the rarefaction wave to travel this distance is

$$t_r \approx \frac{1}{2}\frac{r^{1/3}R_i}{c_s} \ .$$

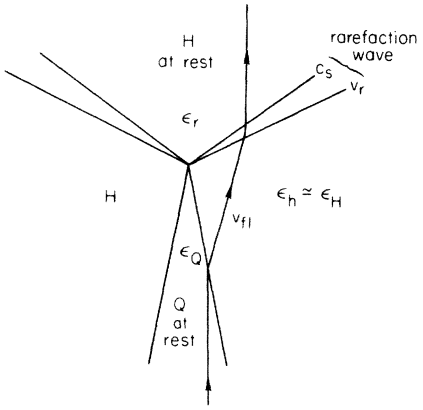

FIG. 22. The death of a quark droplet produces a rarefaction wave which leaves behind a region of lower density.

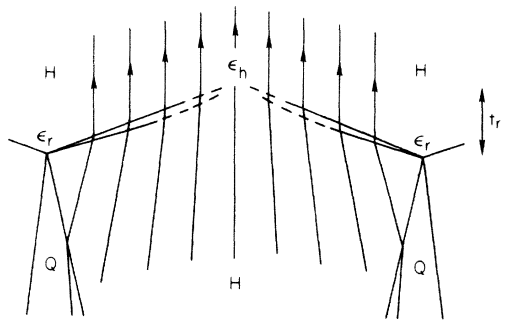

FIG. 23. The rarefaction waves disappear as they enter regions of slower flow. Finally we are left with alternating high- and low-density regions.

During this time the red-shift has reduced the temperature at the droplet decay site by an additional

$$\frac{\Delta T}{T_c}=\left[\frac{\epsilon}{3}\right]^{1/2} t_r=\frac{3r^{1/3}}{2\sqrt{r-1}}\chi R_i$$

corresponding to a density loss

$$\frac{\Delta\epsilon}{\epsilon}=r^{1/3}\frac{6}{\sqrt{r-1}}\chi R_i \ .$$

Thus we are left with alternating high- and low-density regions with a density difference

$$\frac{\Delta\epsilon}{\epsilon}=r^{1/3}\frac{12}{\sqrt{r-1}}\chi R_i$$
$$=1.1\times10^{-3}\left[\frac{T_c}{200\ \text{MeV}}\right]^2\frac{R_i}{1\ \text{m}}$$

(the numerical value is for $r=3$). The inhomogeneity produced is proportional to the nucleation scale R_i, i.e., to the supercooling $(T_c-T_{\rm PT})/T_c$. Supercooling by a few percent will only lead to an inhomogeneity of 10^{-3}. This would persist until the nucleosynthesis era, but with this magnitude its effect on nucleosynthesis is none. Acoustic damping would smooth it out before recombination, so it will not affect the microwave background. If the actual supercooling were larger, $\chi R_i\approx1$, the density fluctuations would correspondingly be larger.

VIII. BARYON NUMBER

As with entropy, the essential constraint here is the conservation of total baryon number. If N_q and N_h are the baryon numbers in the Q and H regions, we thus have

$$\dot N_q(t)=-\dot N_h(t) \ , \tag{8.1}$$

where

$$\dot N_q(t)=\dot n_q(1-h)R^3-n_q\frac{3R^2\dot R}{r-1} \ ,$$
$$\dot N_h(t)=\dot n_h hR^3+n_h3R^2\dot R\frac{r}{r-1} \ . \tag{8.2}$$

We thus have one equation for the two quantities and further assumptions are needed to solve the problem.

As a first example, consider the hydrodynamic transfer of matter. According to Eq. (7.4) then $n_q/n_h=r$ and Eqs. (8.1) and (8.2) are seen to imply that further both n_q and n_h are constant. Expansion does not dilute the densities. Instead, the increase in volume is obtained by converting matter from the dense Q phase to the dilute H phase. Baryon-number density behaves like s.

If s and n are related to T and μ, some difference appears, however. The entropy density s jumps from s_Q to s_H and the temperature from $T_q=T_c$ to T_h so that the difference T_h-T_c is tiny [Eq. (7.3)]. The situation with n and μ is shown in Fig. 24. According to Eq. (2.7) $n_q/n_h=r$ implies that

$$\frac{\mu_q}{\mu_h}=\frac{rb_0}{\frac{1}{9}N_F{T_0}^3} \ , \tag{8.3}$$

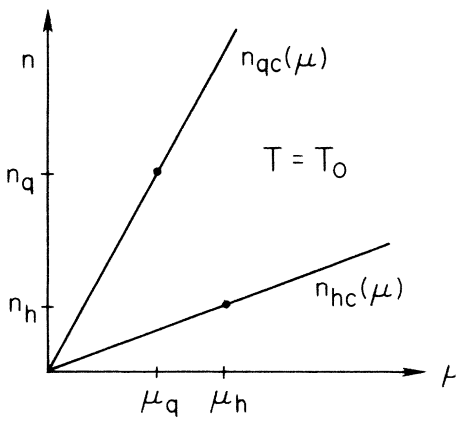

FIG. 24. The net baryon-number density along the critical curve (Fig. 2) as a function of μ in the quark phase (n_{qc}) and in the hadron phase (n_{hc}).

where T_0 is the transition temperature at $\mu>0$ (now we include the contribution of the nucleons to the equation of state for the hadron phase). The chemical potential therefore increases by a factor of 2–4 when crossing the deflagration front.

As a second alternative, assume that the transport mechanism is such that it transports only entropy but no baryon number. This is the case if the radiative enthalpy flux

$$F_{\rm rad}=\frac{g_\nu+g_e+g_\gamma}{g_{\rm hadron}+g_\nu+g_e+g_\gamma}w_H\frac{T_c-T_h}{T_h} \tag{8.4}$$

dominates. Then no baryon number is transmitted through the surface and all the baryon number originally within the Q region remains there, i.e., $\dot N_q=0$. Solving this equation from (8.2) one obtains

$$\frac{n_q(t)}{n_q(t_i)}=\left[\frac{1-\frac{r-1}{r}h(t)}{1-h(t)}\right]^{r-1} \ . \tag{8.5}$$

The resulting $n_q(t)$ thus grows rapidly with t. The apparent singularity of (8.5) near the end of the phase transition is unphysical. The maximum value n_q can have is s_Q and this would happen at

$$1-h(t)=\frac{1}{r}\left[\frac{n_q}{s_Q}\right]^{1/(r-1)}=10^{-5} \ .$$

Then all the baryon number within the initial quark droplet volume ${R_i}^3$ would be condensed to a quark nugget of approximately nuclear matter density.[9] We have here given a kinematic description of what could be happening; it is a much more demanding problem to give a dynamic reason for why this should happen.

One could also try to compute $n_h(t)$, which must decrease, since all the baryon number stays within Q. This quantity, however, depends on what happens within the initial singularity and is incalculable within the present approach. The difficulty is analytically seen in that an integral over dh/h appears in the integration of $\dot N_h=0$.

We have here studied how a quark nugget could be produced if the properties of the Q-H interface are such as to suppress transmission of baryon number. Cosmologically as important a question is also whether these nuggets can be preserved in the hot environment after the quark-hadron transition.[11,31,32] The dynamical properties of the interface play a significant role here, too, and it would seem to us that if the nuggets can be formed they can also be kept.

IX. SEQUENCE OF EVENTS IN A THREE-DIMENSIONAL CONFIGURATION

In earlier sections we resorted to an unrealistic but easily calculable plane-symmetric phase separation configuration. In reality the bubbles and droplets are spherical and this complicates the sequence of events.

The small-supercooling—phase-separation scenario begins with a brief period of bubble nucleation, deflagration, and shock-front collisions. The structure of a spherical deflagration bubble[23] is different from a plane-symmetric bubble (slab). The shock front itself is fairly weak, but it is followed by a wave with increasing density. Thus the simple shock collisions and reflections of Sec. V are replaced by weak collisions followed by a longer period of increasing flows rushing against each other. The detailed study of these events would be a nontrivial task, especially because of the complicated geometry. However, this should not be relevant to the end result. After sloshing around for awhile, the Q region has reheated back to the critical temperature and settled down. The further evolution is governed by the expansion.

For simplicity we assume an idealized situation, in which all the H bubbles have the same size and are distributed, e.g., in a hexagonal or cubic close-packing configuration, with equal initial distances R_i between centers of nearest neighbors. These bubbles are surrounded by a connected Q region and will grow until they meet each other. This is followed by a rearrangement when the Q region becomes disconnected and forms shrinking droplets surrounded by a connected H region (Fig. 25).

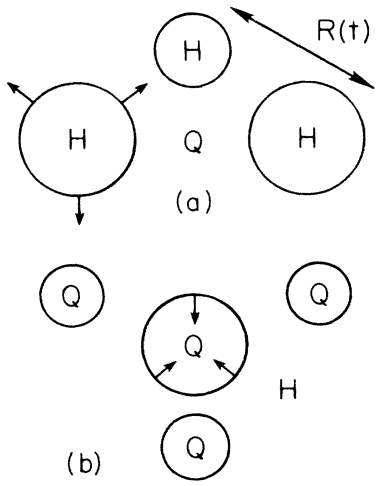

FIG. 25. The phase-separation boundary in the three-dimensional case. The bubble configuration (a) of the early stage of the phase transition changes to a droplet configuration (b) in the late stage.

In this configuration there is one bubble per volume $R(t)^3/\sqrt{2}$. The radius $\rho_h(t)$ of the bubbles is related to their volume fraction [Eq. (3.8)] by

$$h(t)=\frac{4\sqrt{2}}{3}\pi\left[\frac{\rho_h(t)}{R(t)}\right]^3 . \tag{9.1}$$

The bubbles fill half the space $[h(t)=0.5]$ when $\rho_h(t)/R(t)=0.44$ and

$$\chi(t-t_i)=\frac{2\sqrt{r-1}}{3}(\arctan\sqrt{4r-1}-\arctan\sqrt{2r+1})$$
$$=0.06 .$$

After this the surface energy would be smaller with a droplet configuration. However, the bubble configuration persists until the bubbles touch $[\rho_h(t)/R(t)=0.5]$ at $h(t)=\sqrt{2}\pi/6=0.74$ and

$$\chi(t-t_i)=\frac{2\sqrt{r-1}}{3}\left[\arctan\sqrt{4r-1}-\arctan\left[\sqrt{4r-1}-2\sqrt{2}\pi\frac{r-1}{3}\right]\right]$$
$$=0.12 .$$

Now both Q and H regions are connected. As the Q region shrinks further it becomes disconnected and forms droplets. These will then assume a spherical shape. The surface energy would further be reduced if the droplets coalesced to form fewer and larger droplets. This is, however, not likely to happen if our scale is already ~ 1 m, since the forces responsible are not strong enough.[9] For the same reason, it takes some time for the droplets to become spherical. After that has happened the droplet radius ρ_q and volume fraction are related by

$$q(t)=1-h(t)=\frac{4\sqrt{2}\pi}{3}\left[\frac{\rho_q(t)}{R(t)}\right]^3 . \tag{9.2}$$

Inverting Eqs. (9.1) and (9.2) gives

$$\rho_h=\left[\frac{3h}{4\sqrt{2}\pi}\right]^{1/3}R ,$$
$$\rho_q=\left[\frac{3q}{4\sqrt{2}\pi}\right]^{1/3}R \tag{9.3}$$

(see Fig. 26).

Assume the enthalpy flux $F_w=w_H v_h=w_Q v_q$ is purely hydrodynamical. In the present geometry it must satisfy

$$F_w 4\pi\rho^2=\frac{dW_h}{dt}=-\frac{dW_q}{dt} , \tag{9.4}$$

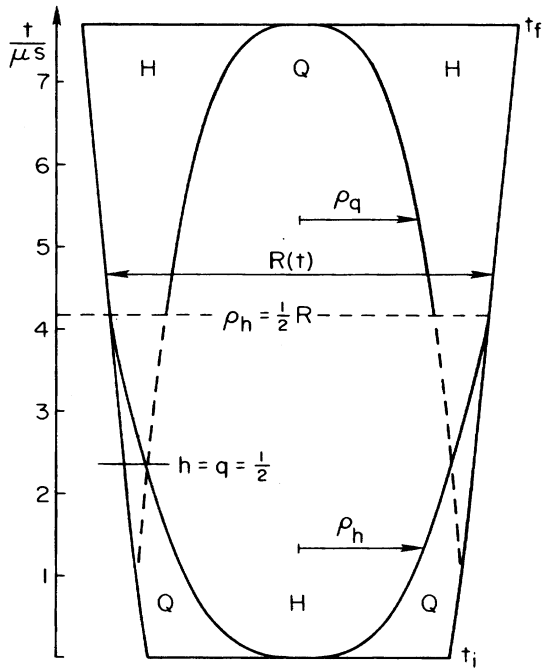

FIG. 26. The evolution of the bubble and droplet sizes according to Eq. (9.3). At $t \approx t_i$ there is a brief period of bubble nucleation and shock collisions not visible in this scale. The bubbles then grow until they touch each other at $\rho_h = \frac{1}{2}R$. The phase boundary then rearranges to form shrinking quark droplets. For behavior close to t see Fig. 28.

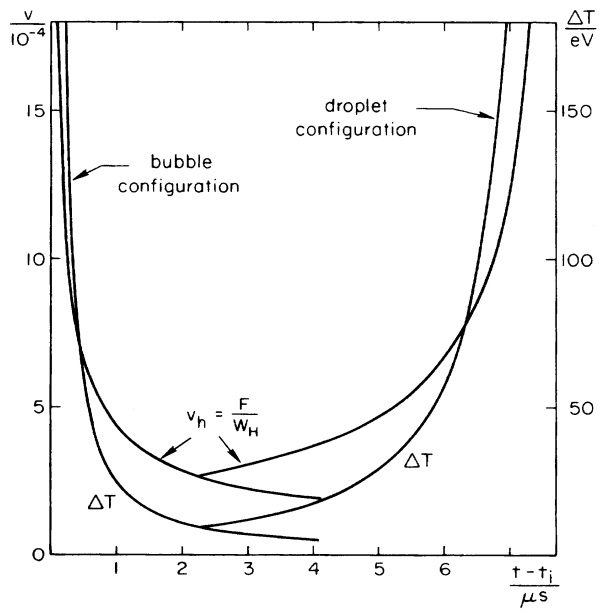

FIG. 27. The flux $F = w_H v_h = w_Q v_q$ (represented in the figure by v_h) between the Q and H regions required to keep them both at the critical temperature, and the required temperature difference ΔT to cause this flux.

where $W = w(\frac{4}{3})\pi\rho^3$ is the enthalpy of one bubble and/or droplet. Since w stays constant, taking a derivative yields

$$v_h = \dot{\rho}, \quad v_q = \frac{1}{r}\dot{\rho} \tag{9.5}$$

for the bubble, and

$$v_q = -\dot{\rho}, \quad v_h = -r\dot{\rho} \tag{9.6}$$

for the droplet. Note that the inside velocity with respect to the surface equals the rate of change of the surface radius. Since density is kept constant, the flow world lines stay at fixed distance from the center point. This is in contrast with the plane-symmetric case where, because of transverse expansion, a flow towards the center plane is needed. Taking a derivative of Eq. (9.3) yields

$$\dot{\rho}_h = \left[\frac{3}{4\sqrt{2}\pi}\right]^{1/3} \frac{\dot{h}R + 3h\dot{R}}{3h^{2/3}}, \qquad \dot{\rho}_q = \left[\frac{3}{4\sqrt{2}\pi}\right]^{1/3} \frac{\dot{q}R + 3q\dot{R}}{3q^{2/3}}, \tag{9.7}$$

where $h,q = 1-h$ and R are from Eqs. (3.8) and (3.9).

From (9.7) it would follow that the bubble growth velocity $\dot{\rho}_h \to$ infinity as $t \to t_i$ and similarly $\dot{\rho}_q \to -$infinity as $t \to t_f$. Clearly some modification is needed close to these end points. For the bubbles this is of no concern, since we treated the initial times already (Secs. IV and V) and noted that the expansion-dominated stage begins only somewhat later. We will next address the droplet decay.

The flux is caused by a small temperature difference $\Delta T = T_c - T_h$ between the Q and H regions [Eq. (7.2)]. The flux velocity and the corresponding temperature difference are shown in Fig. 27. This difference implies $w_h < w_H$. In calculating the required flux we approximated $w_h = w_H$. As $t \to t_f$, ΔT grows large and this approximation is no longer valid. On the other hand, in reality the H region cannot cool faster than the expansion rate. What happens is that, since the H region is no longer maintained at w_H, the required flux is actually lower than what we calculated. Thus the droplet shrinks slower and more time elapses, causing a cumulative time error in our approximation. The time $t = t_f$ is actually passed in a situation where small droplets still remain. As the droplets get small, the flux from them becomes insignificant and the cooling of the H region becomes dominated by the expansion.

Finally we can make another approximation, where we first ignore the droplets in calculating the expansion factor $R(t)$ and the temperature of the H region. According to Eq. (7.2) the droplet will shrink at a rate

$$\dot{\rho}_q = -\left[\frac{1}{r(r-1)}\right]^{1/2} \frac{\Delta T}{T_c}. \tag{9.8}$$

Using ΔT from Eq. (3.12) the droplet radius is then given by

$$\rho_q(t)=\rho_q(t_1)-\frac{1}{\sqrt{r(r-1)}}\int_{t_1}^{t}\left\{1-\left[1+\left[\frac{12}{r-1}\right]^{1/2}\chi(t'-t_f)\right]^{-1/2}\right\}^{1/2}dt'$$

$$=\rho_q(t_1)-\frac{1}{8\sqrt{3r}\chi}\{x(x^2-1)^{1/2}-\ln[x+(x^2-1)^{1/2}]\}_{t_1}^{t}\,, \tag{9.9}$$

where

$$x=2\left[1+\left[\frac{12}{r-1}\right]^{1/2}\chi(t-t_f)\right]^{1/2}-1\,.$$

Using

$$\Delta T(t)\approx\left[\frac{3}{r-1}\right]^{1/2}\chi(t-t_f)T_c\,, \tag{9.10}$$

we get a simpler formula

$$\rho_q(t)\approx\rho_q(t_1)-\frac{1}{\sqrt{r(r-1)}}\left[\frac{12}{r-1}\right]^{1/4}\frac{1}{3\chi}\{[\chi(t-t_f)]^{3/2}-[\chi(t_1-t_f)]^{3/2}\}\,. \tag{9.11}$$

Here $t_1>t_f$ is some initial time when our new approximation becomes valid.

We call our earlier approximation "volume dominated" (VD; required flux determined from change of volumes of the regions) and the new approximation "red-shift dominated" (RD; flux determined by temperature difference caused by red-shift). We switch from VD to RD keeping ΔT constant. The time $t<t_f$ is replaced by a time $t_1>t_f$, solved from (9.10) so as to give the same ΔT. This jump Δt is a first approximation to the cumulative time error mentioned earlier.

Both approximations make an error in the average enthalpy density. In VD we use

$$w_h\approx w_H=g_h4\pi^2\frac{T_c^{\,4}}{90}$$

instead of

$$w_h=g_h4\pi^2\frac{(T_c-\Delta T)^4}{90}$$

and make an error

$$\delta w_{(1)}\approx 4\Delta T\frac{w_H}{T_c}=4r(r-1)v_q{}^2w_H \tag{9.12}$$

too much. In RD we ignore the higher enthalpy of the droplet and make an error

$$\delta w_{(2)}\approx q(w_Q-w_H) \tag{9.13}$$

too little. We can think of this loss of enthalpy density $\delta w_{(1)}+\delta w_{(2)}$ as being due to the expansion during Δt. We can express both errors in terms of q:

$$\frac{\delta w_{(2)}}{w_H}\approx q(r-1) \tag{9.14}$$

and

$$\frac{\delta\omega_{(1)}}{w_H}\approx r(r-1)\left[\frac{3\sqrt{2}}{\pi}\right]^{2/3}\frac{(q\dot{R}+\frac{1}{3}\dot{q}R)^2}{q^{4/3}}\,, \tag{9.15}$$

where

$$-(q\dot{R}+\tfrac{1}{3}\dot{q}R)=\left[\frac{r}{1+(r-1)q}\right]^{1/3}\frac{\sqrt{3+4(r-1)q}}{(r-1)^{3/2}}\chi R_i$$

$$\approx\frac{r^{1/3}}{(r-1)^{3/2}}\sqrt{3}\chi R_i\,.$$

Thus $\delta w_{(1)}$ grows and $\delta w_{(2)}$ shrinks as $q\to 0$. We minimize the error by making the switch when $\delta w_{(1)}=\delta w_{(2)}$ which yields

$$q(t_1)=\left[\frac{486r^5}{\pi^2(r-1)^9}\right](\chi R_i)^{6/7}\,. \tag{9.16}$$

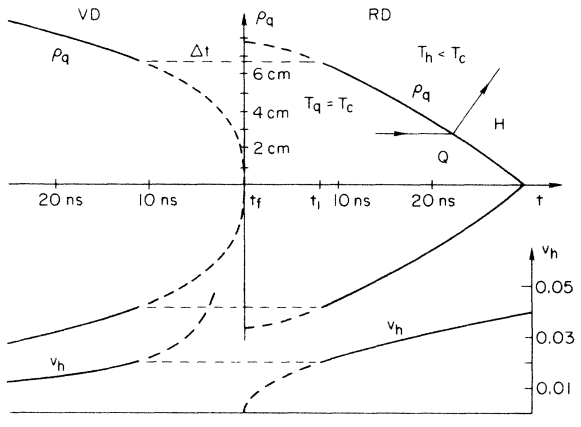

FIG. 28. The last stages of a (3D) quark droplet. This figure is for $R_i=1$ m. The figure shows the switch between our two approximations. The curves left of t_f show droplet size and velocity v_h in the VD approximation (see the text). v_h is proportional to the square of the temperature difference ΔT between the two phases. As ΔT and v_h grow, this approximation becomes worse giving too fast shrinkage. Thus, the last moments are treated in the RD approximation, which is good when the droplet is sufficiently small.

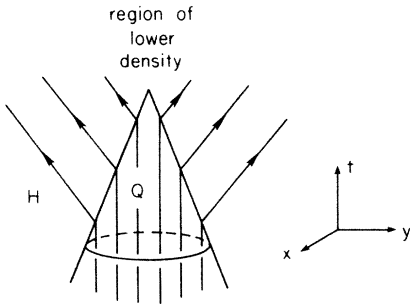

FIG. 29. The flow patterns near the death of the (3D) quark droplet.

In Fig. 28 we show the final stage of the quark droplet as described above. Using the reference values $r=3$, $\chi=1/10\,780$ m, and $R_i=1$ m, we have $q(t_1)=0.000\,56$, which corresponds to a droplet radius $\rho(t_1)=6.5$ cm.

In VD this radius is reached at $t=t_f-10.6$ nsec. More important, the droplet is then shrinking at the rate $-\dot{\rho}=0.0068=2.0$ mm/nsec, corresponding to a temperature difference $\Delta T/T_c=0.000\,27$. In RD this ΔT is reached at $t=t_i=t_f+8.0$ nsec.

As we now let the expansion determine the cooling of the H region and thus the shrinking rate of the droplet, it takes an additional 21.2 nsec for a droplet of radius 6.5 cm at $t=t_f+8.0$ nsec to die. The final velocities are

$$v_q=0.013=4 \text{ mm/nsec},$$

$$v_h=0.039=12 \text{ mm/nsec}.$$

Since the fluid is flowing outwards with a velocity v_h-v_q, the flow will leave behind a rarefied region after the droplet has decayed (Fig. 29). We have not done a quantitative study of the following evolution, which would involve spherical rarefaction waves. Note, however, that the final velocities are about 100 times larger than in the planar case. This implies much sharper inhomogeneities.

X. CONCLUSION

Obtaining a detailed picture of the sequence of events during the quark-hadron phase transition era of the early Universe at $t\sim 10$ μsec would be very important cosmologically. In particular, one would hope to be able to compute the resulting inhomogeneities and concentrations of baryon number. Unfortunately, QCD is so complicated a theory that we have only little first-principles information on the equation of state and none at all on the kinetics of the transitions. Thus one has to resort to a study of models and scenarios.

We have studied the small-supercooling—phase-separation scenario in detail. In this scenario, there is first a short period of initial supercooling and bubble nucleation. The bubbles grow and the shock waves preceding them collide. After a while the turbulence dies out and the Universe settles in a state in which there are small hadron bubbles immersed in quark matter at $T=T_c$. The essential parameter characterizing this stage is a new scale appearing in the problem: the average distance R_i between the bubbles. The consequences of this scenario are as a rule proportional to χR_i, the ratio between R_i and the Hubble distance $1/\chi$. We estimate that, on the average, $\chi R_i\sim 10^{-4}$. However, even larger values cannot be excluded.

After the short initial period the expansion of the Universe continues at fixed temperature and pressure by converting more and more matter from the denser Q to the less dense H phase until all the matter is in the form of hadrons. The sequence of events can be discussed in detail and various quantities describing it can be expressed as functions of χR_i.

The crucial question, of course, is what effects remain after the transition is over. A fairly reliable prediction is that there will be a density inhomogeneity

$$\frac{\Delta\epsilon}{\epsilon}\sim\chi R_i$$

concentrated at the positions of the initial hadron bubbles. On the average, this is of the order of 10^{-3}, but again, if large supercoolings can be sustained, R_i approaches the Hubble scale $1/\chi$ and correspondingly larger inhomogeneities will be produced.

A particularly important but very speculative question is that of enrichment of baryon number in the Q droplets. Even in the framework of hydrodynamic matter transfer, this is a dynamical question depending on the properties of the quark-hadron interface. We analyzed the enrichment in the two limits of complete transparency and intransparency relative to transfer of net baryon number. It seems possible that if the properties of the surface are such that quark nuggets are formed, they will also survive the hot period after the phase transition.

Before we can make definite predictions of the consequences of the cosmological quark-hadron phase transition, both considerable theoretical and experimental advances are needed. Although the little bang formed in ultrarelativistic nuclear collisions is so totally different from the Universe at $T\sim 200$ MeV as far as size, isotropy, homogeneity, and net baryon number are concerned, the forthcoming nuclear collision experiments should shed much new light on these questions.

ACKNOWLEDGMENTS

We thank Tom DeGrand for collaboration at the early stages of this work. H. Kurki-Suonio gratefully acknowledges financial support from the Jenny and Antti Wihuri Foundation and the Academy of Finland.

[1]For a review of the present state of quark matter physics, see *Quark Matter '84,* proceedings of the Fourth International Conference on Ultrarelativistic Nucleus-Nucleus Collisions, Helsinki, 1984, edited by K. Kajantie (Lecture Notes in Physics, Vol. 221) (Springer, Berlin, 1985).
[2]K. Olive, Nucl. Phys. **B190**, 483 (1981).
[3]E. Suhonen, Phys. Lett. **119B**, 81 (1982).
[4]M. Crawford and D. Schramm, Nature (London) **298**, 538 (1982).
[5]E. Kolb and M. Turner, Phys. Lett. **115B**, 99 (1982).
[6]J. Lodenquai and V. Dixit, Phys. Lett. **124B**, 317 (1983).
[7]C. Hogan, Phys. Lett. **113B**, 172 (1983).
[8]T. DeGrand and K. Kajantie, Phys. Lett. **147B**, 273 (1984).
[9]E. Witten, Phys. Rev. D **30**, 272 (1984).
[10]S. Midorikawa, Phys. Lett. **158B**, 107 (1985).
[11]J. Madsen and K. Riisager, Phys. Lett. **158B**, 208 (1985).
[12]J. H. Applegate and C. Hogan, Phys. Rev. D **31**, 3037 (1985).
[13]T. DeGrand, T. W. Kephart, and T. J. Weiler, Phys. Rev. D **33**, 910 (1986).
[14]K. Iso, H. Kodama, and K. Sato, Phys. Lett. **169B**, 337 (1986).
[15]J. D. Bjorken, Phys. Rev. D **27**, 140 (1983).
[16]L. Van Hove, Phys. Lett. **118B**, 138 (1982).
[17]K. Kajantie, R. Raitio, and P. V. Ruuskanen, Nucl. Phys. **B222**, 152 (1983).
[18]G. Baym, B. Friman, J.-P. Blaizot, M. Soyeur, and W. Czyz, Nucl. Phys. **A407**, 541 (1983).
[19]B. Friman, K. Kajantie, and P. V. Ruuskanen, Nucl. Phys. **B266**, 468 (1986).
[20]H. von Gersdorff, L. McLerran, M. Kataja, and P. V. Ruuskanen, Phys. Rev. D **34**, 794 (1986).
[21]K. Kajantie, M. Kataja, L. McLerran, and P. V. Ruuskanen, Phys. Rev. D **34**, 811 (1986).
[22]M. Gyulassy, K. Kajantie, H. Kurki-Suonio, and L. McLerran, Nucl. Phys. **B237**, 477 (1984).
[23]H. Kurki-Suonio, Nucl. Phys. **B255**, 231 (1985).
[24]L. Van Hove, Z. Phys. C **21**, 93 (1983).
[25]L. Van Hove, Z. Phys. C **27**, 135 (1985).
[26]V. Dixit and E. Suhonen, Z. Phys. C **18**, 355 (1983).
[27]U. Heinz, P. Subramanian, H. Stocker, and W. Greiner, Brookhaven National Laboratory Report No. BNL-37016, 1985 (unpublished).
[28]J. Cleymans, K. Redlich, H. Satz, and E. Suhonen, Bielefeld report, 1986 (unpublished).
[29]R. Courant and K. Friedrichs, *Supersonic Flow and Shock Waves* (Springer, Verlag, 1976).
[30]L. D. Landau and E. M. Lifshitz, *Course of Theoretical Physics,* Vol. 6, *Fluid Mechanics* (Pergamon, New York, 1959), Sec. 126.
[31]C. Alcock and E. Farhi, Phys. Rev. D **32**, 1273 (1985).
[32]J. Madsen, H. Heiselberg, and K. Riisager, Aarhus report, 1986 (unpublished).